

Triggered Drug Release from an Antibody–Drug Conjugate Using Fast “Click-to-Release” Chemistry in Mice

Raffaella Rossin,[†] Sander M. J. van Duijnhoven,[†] Wolter ten Hoeve,[‡] Henk M. Janssen,[§] Laurens H. J. Kleijn,[§] Freek J. M. Hoeben,[§] Ron M. Versteegen,[§] and Marc S. Robillard^{*,†}

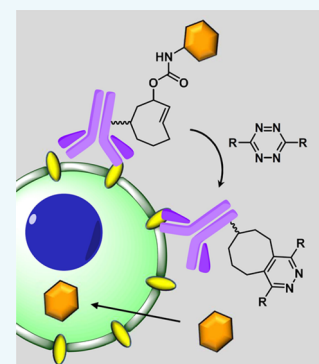
[†]Tagworks Pharmaceuticals, High Tech Campus 11, 5656 AE Eindhoven, The Netherlands

[‡]Syncom, Kadijk 3, 9747 AT Groningen, The Netherlands

[§]SyMO-Chem, Het Kranenveld 14, 5612 AZ Eindhoven, The Netherlands

Supporting Information

ABSTRACT: The use of a bioorthogonal reaction for the selective cleavage of tumor-bound antibody–drug conjugates (ADCs) would represent a powerful new tool for ADC therapy, as it would not rely on the currently used intracellular biological activation mechanisms, thereby expanding the scope to noninternalizing cancer targets. Here we report that the recently developed inverse-electron-demand Diels–Alder pyridazine elimination reaction can provoke rapid and self-immolative release of doxorubicin from an ADC in vitro and in tumor-bearing mice.



INTRODUCTION

Antibody–drug conjugates (ADCs) are highly potent biopharmaceuticals that use the targeting ability of antibodies (mAbs) to selectively bind to tumor cells where the conjugated drug is released.¹ This allows the use of drugs that would normally be too toxic. Current clinically established ADCs have to bind to a tumor cell-specific membrane receptor and subsequently be internalized in the tumor cell for biological cleavage of the linker—and thus activation of the drug—to occur. As the number of tumor-specific receptors that ensure efficient internalization is limited, especially in solid tumors,² a wide range of cancer targets remains out of reach of current ADCs. There are many noninternalizing receptors or extracellular matrix markers that are abundantly and selectively present in many solid cancers.^{3–6} These would be superb targets for ADC therapy if there were a way to selectively release the drug from the antibody extracellularly. Therefore, we set out to develop an ADC linker that can be chemically triggered to release its potent cargo. In this approach, after the ADC has bound to an extracellular cancer target and unbound ADC has cleared from blood, an activating probe is administered that reacts with the ADC linker via a fast click reaction to liberate and activate the drug. As many currently used ADC drugs are cell permeable,¹ it is expected that the released drug will penetrate and kill surrounding cancer cells. Recently, Neri and co-workers achieved good therapeutic efficacy in tumor-bearing mice using a noninternalizing ADC that relies on cleavage of a disulfide linker by extracellular thiols.⁵ However, compared to biological release mechanisms, a

bioorthogonal ADC activation approach may allow a more direct control over drug release in vivo.

We and others have demonstrated that the fastest click reaction, the inverse-electron-demand Diels–Alder (IEDDA) reaction,^{7,8} can be used for pretargeted radioimmunoimaging, treating tumor-bearing mice with *trans*-cyclooctene (TCO)-tagged mAb or mAb fragments, followed 1–3 days later by administration and selective conjugation of a radiolabeled tetrazine probe to the TCO tag of the tumor-bound antibody.^{6,9–13}

Recently, we have developed a new reaction, which we termed the IEDDA pyridazine elimination, a “click-to-release” approach that affords instantaneous and selective release upon conjugation (Figure 1 and Scheme 1a).¹⁴ IEDDA reactions afford 4,5-dihydropyridazines (7), which usually tautomerize to 1,4-dihydropyridazines (8 and 9). We demonstrated that the 1,4-dihydropyridazine product 9 derived from a TCO containing a carbamate-linked doxorubicin (Dox) at the allylic position (1) and tetrazine (2–4) is prone to eliminate CO₂ and Dox via a novel electron cascade mechanism affording pyridazine 10, which then rearranges to aromatic pyridazine 11 (Scheme 1a).

Owing to the increased electron density, 3,6-dimethyl-1,2,4,5-tetrazine (3) and 3-(2-pyridyl)-6-methyl-1,2,4,5-tetrazine (4) were approximately 100- and 10-fold less reactive than

Received: May 9, 2016

Revised: June 13, 2016

Published: June 15, 2016

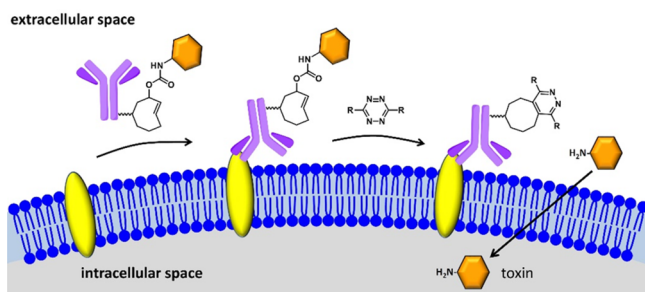


Figure 1. Antibody–drug conjugate activation with “click-to-release” chemistry on a tumor cell.

3,6-bis(2-pyridyl)-1,2,4,5-tetrazine (**2**), which we used for pretargeting in vivo. Conversely, **2** gave almost no Dox release (7%), whereas **3** and **4** instantaneously afforded free drug in 55% and 79% yield, respectively, in PBS, serum, and cell culture. This unprecedented finding in a prodrug context holds great promise for a range of applications in medicine, chemical biology, and synthetic chemistry, including triggered drug release, biomolecule uncaging, and capture and release strategies. Since then the IEDDA pyridazine elimination reaction has been used for nanoparticle-based prodrug activation,¹⁵ intracellular uncaging of enzymes in vitro and in vivo,^{16,17} and the purification of solid-phase synthesized oligonucleotides.¹⁸

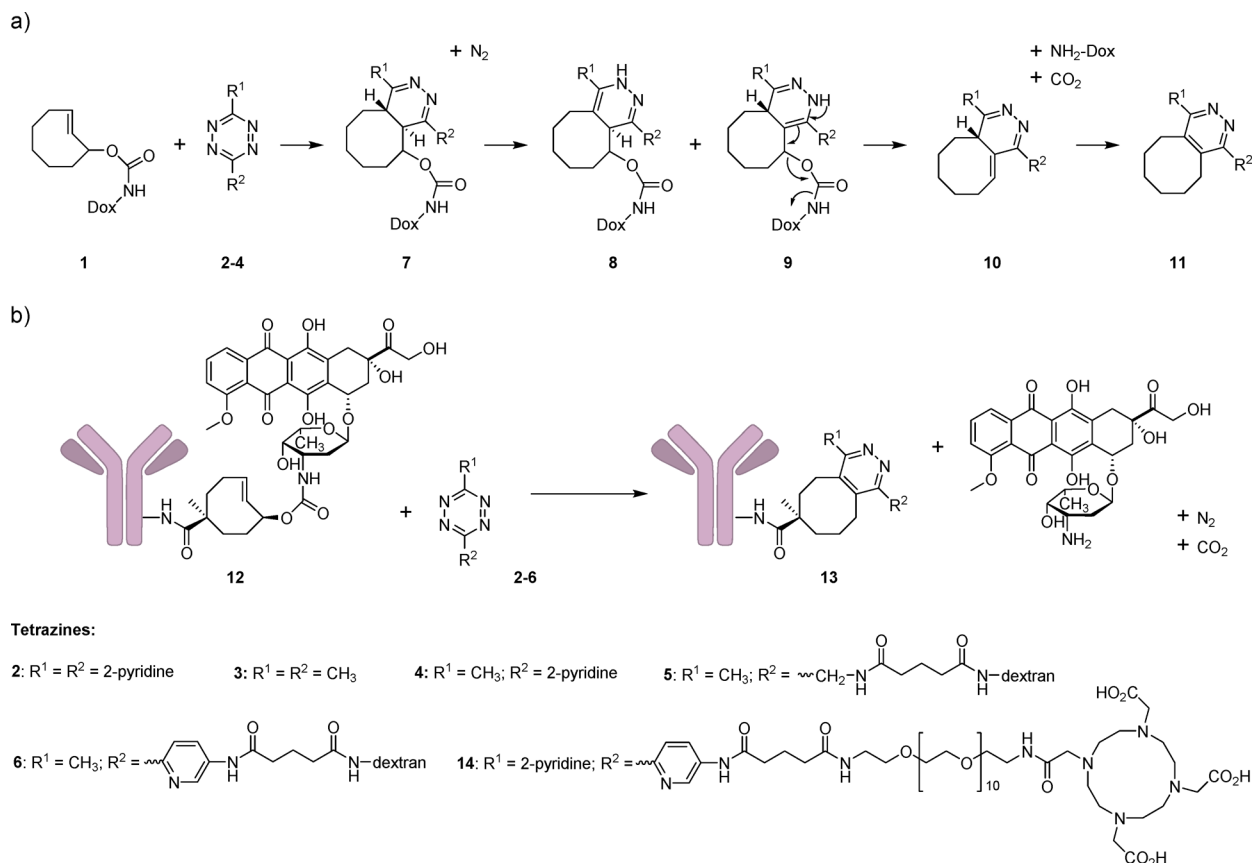
For a future application in ADC therapy we reasoned that it is necessary to first demonstrate tumor targeting of a model ADC comprising a TCO-linked model drug and quantify and

optimize its tetrazine-induced activation and resulting drug release in vivo. For this proof of principle study we set out to use the anti-TAG72 mAb CC49 and link it via TCO to the intrinsically fluorescent Dox as a detectable model drug for the more potent toxins typically used in ADCs. TAG72 does not internalize, has slow shedding, and is highly overexpressed in a wide range of solid cancers. The TAG72/CC49 couple has been used in the clinic for (pretargeted) radioimmunotherapy^{19,20} and by us for preclinical IEDDA pretargeting,^{11,12,21–23} providing a strong rationale for developing chemically activated ADCs for this system. This present report is the first example of a click-chemistry activatable ADC and demonstrates high tumor uptake of the ADC, its direct chemically controlled activation and good tumor retention of the released model drug, setting the stage for future therapy studies.

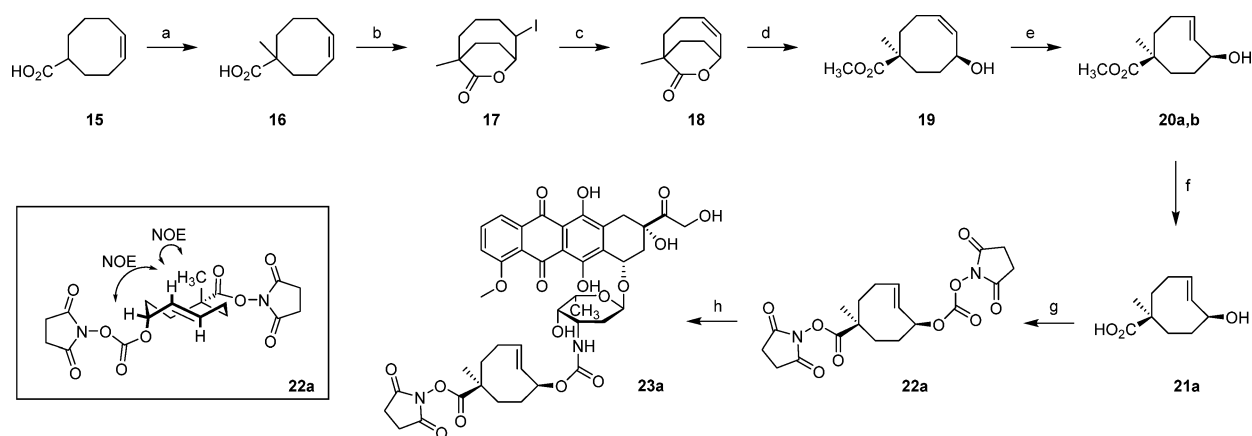
RESULTS AND DISCUSSION

A suitable synthesis route toward an analog of TCO **1** that can be conjugated to a mAb should meet two requirements. It should afford facile isolation of diastereoisomers with the conjugation handle on the TCO in either the equatorial or the axial position and with an allylic hydroxyl in the axial position, as the equatorial hydroxyl-derived carbamate was previously shown to be 156-fold less reactive,¹⁴ due to steric hindrance and, possibly, electronic effects.²⁴ In addition, it should allow subsequent orthogonal manipulation of the conjugation handle and the hydroxyl. We designed a route centering on the iodolactonization of 4-cyclooctene-1-carboxylic acid **16** followed by hydrogen iodide elimination and lactone hydrolysis to

Scheme 1. (a) Proposed Mechanism for the IEDDA Pyridazine Elimination between a Doxorubicin-Functionalized *trans*-Cyclooctene (TCO) and a Tetrazine. (b) mAb-TCO-Doxorubicin and Activators Used in the Study



Scheme 2. Synthesis of NHS-*trans*-Cyclooctene-Doxorubicin 23a (a: Hydroxyl and Derivatives in Axial Position, As Determined by NOESY NMR)^a



^aReagents/conditions: (a) 1. Diisopropylamine, *n*-butyllithium; 2. iodomethane, THF/hexanes, -50 to $+50$ °C, 100%; (b) NaHCO₃, KI, I₂, DCM/H₂O, 0 °C; (c) DBU, toluene, reflux, 94%; (d) KHCO₃, MeOH, 28 °C, 48%; (e) methyl benzoate, UV, heptane/ether, RT, 72%; (f) KOH, MeOH, 28 °C, 75%; (g) DIPEA, *N,N'*-disuccinimidyl carbonate, MeCN, RT, 46%; (h) doxorubicin HCl, DIPEA, DMF, 20 °C, 68%.

stereoselectively install the hydroxyl in the allylic position, eventually affording bis-NHS-activated linker **22a** (Scheme 2).

We introduced a methyl group near the carboxylic acid of **15**, affording **16**, to prevent epimerization during lactone hydrolysis and to enable regioselective conjugation of **22a** with Dox. Iodolactonization gave **17** as a single isomer, and subsequent hydrogen iodide elimination resulted in enolactone **18**. Hydrolysis gave the desired ring-opened **19** with the hydroxyl positioned *cis* relative to the methyl ester. UV irradiation of **19** afforded a mixture of the two possible TCO isomers with the hydroxyl respectively in the axial (**20a**) and equatorial (**20b**) position and the methyl ester respectively in the equatorial (**20a**) and axial (**20b**) positions, as evidenced by NOESY NMR. We were pleased to find that only **20a** underwent hydrolysis to carboxylic acid **21a**, thus enabling a straightforward separation between both isomers. Activation to the bis-NHS derivative **22a** and subsequent reaction with 1 equiv Dox afforded the desired selective reaction with the NHS-carbonate vs the sterically hindered NHS-ester, leading to axial NHS-TCO–Dox **23a**.

To compensate for the steric hindrance imparted by the methyl group next to the NHS ester, we reacted an excess of 40 equiv **23a** with CC49 via Lys residues to obtain >95% monomeric and immunoreactive CC49-TCO-Dox conjugate **12** with a drug-to-antibody ratio of ca. 2 (Scheme 1). TCO can isomerize to the unreactive *cis*-isomer due to several causes including contact with copper-containing serum proteins.²³ The isomerization of **12** was followed in stock (PBS, 4 °C) over one year and the extrapolated data indicate an exceptionally long shelf life for the *trans* isomer ($t_{1/2}$ = 2.6 years). Moreover, no spontaneous Dox release was observed in that time, as confirmed by fluorescence RP-HPLC analysis.

The *in vivo* behavior of **12** was assessed in biodistribution studies after labeling the protein directly with ¹²⁵I. In mice the circulation in blood for **12** ($t_{1/2}$ = 26.9 h) was similar to that of native CC49 ($t_{1/2}$ = 26.3h¹¹) (Figure 2a) and a similar biodistribution was observed 4 days post-mAb injection (Table S2) indicating that the 2 TCO–Dox moieties did not perturb the mAb. The serum protein induced isomerization and deactivation of the TCO linker comprised in **12** in circulation was assessed by reacting blood samples with an excess ¹⁷⁷Lu-14

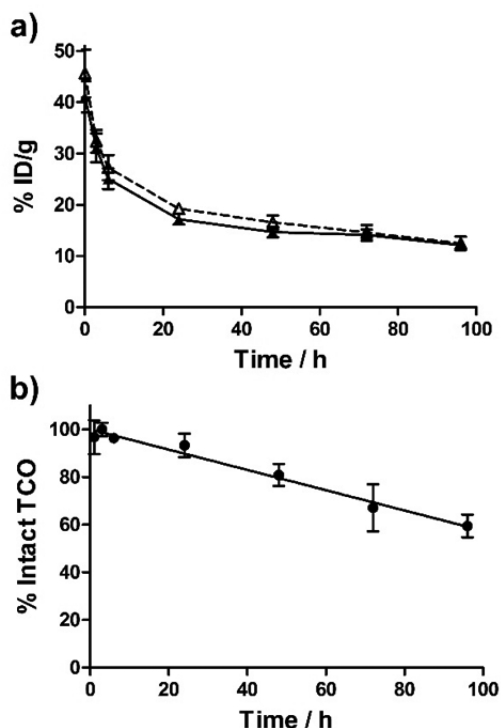


Figure 2. (a) Blood clearance of ¹²⁵I-CC49-TCO-Dox (solid line) and ¹²⁵I-CC49 (dashed line, from Rossin et al.¹¹) and (b) *in vivo* stability of the TCO linker in ¹²⁵I-CC49-TCO-Dox in tumor-free mice (obtained by taking blood samples containing ¹²⁵I-CC49-TCO-Dox and reacting *ex vivo* with an excess of ¹⁷⁷Lu-DOTA-tetrazine, followed by size exclusion purification and dual-isotope gamma counting to evaluate the change of reaction yield with time). Data represent the mean with one SD ($n = 3$).

ex vivo followed by size exclusion purification and dual-isotope gamma counting (¹⁷⁷Lu/¹²⁵I ratio). With this procedure we measured a stability half-life of 5 days for the TCO (Figure 2b), which is comparable to that of other TCOs²³ and to the cleavage half-lives of conventional cleavable ADC linkers.²⁵ In contrast to the latter, TCO isomerization only results in loss of reactivity, not in payload release (Figures S5 and S6).¹⁴

In vitro drug release was evaluated either by detecting the amount of residual Dox attached to the mAb (SEC HPLC with UV measurements at 480 nm for Dox and 260 nm for the protein, Figure S4) or by quantifying the amount of free Dox in solution (fluorescence RP-HPLC with Daun as internal standard, Figures 3, S5 and S6, and Table S1) at various

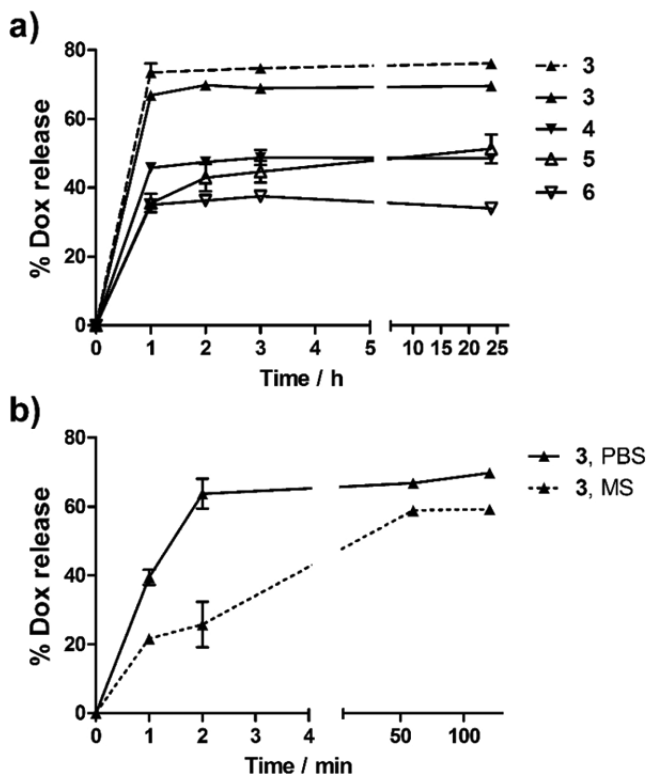


Figure 3. Dox release from (a) CC49-TCO-Dox 12 (1–3 μM) upon reaction with activators 3–6 in PBS at 37 °C: solid lines from RP-HPLC, dashed line from SEC-HPLC. (b) 12 (1 μM) upon reaction with 3 in PBS (solid line) and 50% mouse serum (MS; dashed line) at 37 °C, from RP-HPLC. RP-HPLC analysis: change in Dox and Daun (internal standard) peak areas; excitation at 485 nm, fluorescence at 590 nm. SEC-HPLC analysis: change in mAb peak area ratio at 480 and 260 nm. The data represent the mean ± SD ($n = 3$).

times post-activation. The Dox release from 12 upon reaction with tetrazines 3 and 4 showed a similar trend to that observed with the model TCO–Dox 1 in our earlier study.¹⁴ We detected fast and high Dox release after reacting 12 (3 μM) and 3 (100 equiv to TCO) in PBS at 37 °C, affording $73.5 \pm 2.6\%$ and $76.1 \pm 0.2\%$ release at 1 and 24 h, respectively (Figure 3a). The amount of free Dox in solution after reaction with 4 was approximately 2/3 of what was released by 3. Slightly lower apparent release was observed in serum (Table S1) due to the fact that liberated Dox was unstable in that medium (Figure S6). Both reactions ran to completion with only ca. 2% of the initial TCO present after 1 h (Table S1). As demonstrated previously,¹⁴ the difference in release yields is due to the difference in electron density of the tetrazines, most likely resulting in a different distribution between the two tautomers 8 and 9, which do not readily interconvert at pH 7 and of which 8 does not release the drug (Scheme 1). The rate of tautomerization from 7 to 8 and 9 and the resulting instantaneous drug release rate appear to depend strongly on the medium. In MeCN the release was previously shown to take several hours, while in PBS it was complete within 1 h.¹⁴

Indeed, when we examined the release reaction between 12 and 3 at shorter time points in PBS, the release was incomplete at 1 min and almost complete at 2 min ($63.8 \pm 4.3\%$, Figure 3b), corresponding to findings in other studies.¹⁶ Interestingly, in serum the release is ca. 2-fold slower, possibly due to a slower tautomerization in this medium (Figure 3b).

The tumor targeting and Dox release from ¹²⁵I-12 upon reaction with activators 3–4 was tested in mice bearing colon carcinoma xenografts (LS174T). A 5 mg/kg dose of 12 gave a high tumor uptake of 30–40%ID/g 30 h post-injection (Table S4). To prevent triggered drug release in blood we used a previously validated albumin-based clearing agent,^{11,21} comprising liver-directing galactose residues and tetrazines 2, which enables rapid reaction with and removal of a TCO-tagged antibody from blood. Importantly, the use of tetrazine 2 does not induce significant drug release.¹⁴ The clearing agent was administered 24 h after ADC 12, followed by the activator 3 or 4 at 26 h. To account for the lower reactivity of 3 and 4 and to achieve complete reaction with the tumor-bound TCO, an excess of the activators (1× dose = 33.5 μmol tetrazine/kg; 10× dose = 0.335 mmol tetrazine/kg) was injected either intravenous (iv) or intraperitoneal (ip) with no signs of acute toxicity (post-injection discomfort, stress, behavioral changes, etc.). Similarly, no decrease in body weight over time was found by Chen and co-workers when injecting higher doses of 3 (1.25 mmol tetrazine/kg, three times a week) in mice to achieve tetrazine-mediated protein uncaging in vivo.¹⁷ To precisely evaluate the in vivo performance of this novel ADC system in this first in vivo study we chose to directly measure the on-tumor reaction between the ADC linker and the tetrazines as well as the resulting drug release instead of evaluating tumor response as a readout of CC49-TCO-Dox activation (Figure 4).

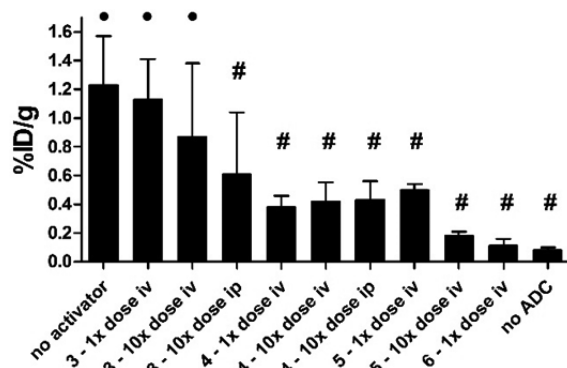


Figure 4. Tumor uptake of ¹⁷⁷Lu-DOTA-tetrazine 14 in mice pretreated with CC49 (no ADC), CC49-TCO-Dox (no activator), or CC49-TCO-Dox followed by activators 3–6, administered at 1× (33.5 μmol tetrazine/kg) or 10× (0.335 mmol tetrazine/kg) dosage, intravenous (iv) or intraperitoneal (ip). One-way ANOVA: $P < 0.0001$; Dunnett's post-test: ● $P < 0.05$, comparison with "no ADC" group; # $P < 0.05$, comparison with "no activator" group. Data represent the mean with one SD ($n = 3–6$).

While relatively few studies have been reported on the quantification of in vivo drug release for the current ADC systems,^{26,27} the nature of the chemically activatable ADC linker makes it well suited for in vivo monitoring of activation through click-chemistry with a radiolabeled probe. After ADC and activator administration, at 27 h we therefore injected the mice with the highly reactive but poorly releasing tetrazine ¹⁷⁷Lu-14 (0.335 μmol tetrazine/kg), which is an analog of 2 and

has been extensively validated in our pretargeting studies.^{11,12,21,22} We then compared the ¹⁷⁷Lu uptake in tumor with a minimum (complete blocking) and maximum (no blocking) value. The minimum tumor uptake ($0.08 \pm 0.02\%$ ID/g), corresponding to the scenario where all tumor-bound TCO has reacted with the activator and is therefore not available for reaction with ¹⁷⁷Lu-14, was obtained by injecting ¹⁷⁷Lu-14 in mice pretreated with native CC49 (“no ADC” group). The maximum tumor uptake ($1.23 \pm 0.34\%$ ID/g) was obtained from mice pretreated with 12 followed only by ¹⁷⁷Lu-14 (“no activator” group).

No significant tumor blocking was observed when the least reactive activator 3 was administered iv at 1× or 10× dosage, probably because of fast clearance leading to insufficient tumor concentrations (Figure 4). Indeed, when the systemic distribution of 3 (10× dose) was slowed down by ip administration, significant but incomplete blocking was observed. Similar results were recently obtained by Chen and co-workers by using a 2-fold higher iv dose of 3 for in vivo intracellular enzyme activation.¹⁷ On the contrary, the more reactive activator 4 produced significant blocking at both dosages already with iv injection, while ip administration did not further improve the reaction yield on tumor. However, the ¹⁷⁷Lu-14 tumor uptake was still above baseline, proving that the on-tumor reaction between TCO and 4 was still incomplete.

To improve the reaction yields, we aimed to further increase the on-tumor reaction time and turned to the use of a slow clearing dextran carrier for the tetrazines.²⁸ Compounds 5 and 6 (Scheme 1), carrying an average of 2.3 tetrazines per molecule, were obtained by conjugating derivatives of 3 and 4 to amine-functionalized 10 kDa dextran. Despite reduced release yields in vitro (Figure 3 and Table S1), possibly due to steric hindrance and microenvironment changes caused by the dextran, we were pleased to find that complete blocking could be achieved without signs of acute toxicity with iv administered 5 (10× dosage) and 6 (1× dosage) (Figure 4), signifying complete on-tumor click reactions. Next, the tumors of these mice were homogenized and extracted to confirm on-tumor drug release. RP-HPLC analysis of the extracts indeed demonstrated the presence of free Dox in tumors treated with 5 and 6, with $44 \pm 11\%$ and $37 \pm 5\%$ recovery, respectively, based on the maximum in vitro release yields and the total amount of 12 in tumors (not corrected for ca. 10% in vivo TCO deactivation in 26 h). Considering the pronounced Dox degradation observed in vivo and in serum in vitro (Figures S9 and S6) and the fact that only intact Dox was quantified, the actual amounts of released Dox in the tumor are likely considerably higher, approaching the maximum release yields found in vitro. For 5 this yield is $51.3 \pm 4.2\%$ after 24 h which compares well with in-tumor release yields determined for conventional ADCs at similar time points.²⁶ Furthermore, the findings suggest that tumor washout, if any, of the extracellular released drug is minimal. Lastly, only very low levels of free Dox was detected in control tumors harvested from mice that only received the ADC ($0.7 \pm 0.2\%$ Dox recovery). This unspecific release is lower than what would be obtained with current cleavable ADC linkers,²⁵ and confirms that the actively triggered drug release is indeed tetrazine dependent.

CONCLUSION

In summary, we have demonstrated the effective use of bioorthogonal elimination chemistry in a living animal, chemically activating a tumor-bound ADC with the recently developed IEDDA pyridazine elimination reaction. The model ADC exhibited excellent tumor uptake, good in vivo stability, and was selectively reactive toward tetrazines, affording efficacious drug release and tumor retention of the drug. This biocompatible approach is ideally suited for use with antibody fragments to eliminate the need for a clearing agent, reducing complexity of the system. The next challenges lie in further increasing the release yield, possibly combined with the use of less bulky plasma half-life extenders than dextran, and to demonstrate therapeutic proof of concept using potent toxins. This “click-to-release” concept for ADCs may circumvent endogenous, intracellular and extracellular, activation mechanisms (i.e., proteases and thiols), thereby potentially expanding the scope to non-internalizing cancer targets, and affording direct control over drug release as opposed to relying on inherently variable cancer biology. In addition it should maximize the bystander effect in heterogeneous tumors, attacking cancer cells that do not express the targeted receptor. As such, we believe click-triggered release may become transformative for ADC therapy and in addition may play an important role in several other fields in vitro and in vivo.

EXPERIMENTAL PROCEDURES

See Supporting Information for general procedures and synthesis of activators 5–6. The syntheses of 3,6-dimethyl-1,2,4,5-tetrazine (3), of 3-(2-pyridyl)-6-methyl-1,2,4,5-tetrazine (4),¹⁴ of 2,2',2''-(10-(2,40,44-trioxo-44-((6-(6-(pyridin-2-yl)-1,2,4,5-tetrazin-3-yl)pyridin-3-yl)amino)-6,9,12,15,18,21,24,27,30,33,36-undecaoxa-3,39-diazatetracontyl)-1,4,7,10-tetraazacyclododecane-1,4,7-triyl)triacetic acid (14),²² of the clearing agent (galactose- and tetrazine-functionalized mouse serum albumin)²¹ and of (Z)-cyclooct-4-ene-1-carboxylic acid (15)²⁹ were reported elsewhere.

(Z)-1-Methylcyclooct-4-ene-1-carboxylic acid (16). A mixture of diisopropylamine (90.2 g, 0.893 mol) and 300 mL THF was cooled to below -20 °C and *n*-butyllithium in hexanes (2.5 N, 360 mL, 0.900 mol) was added slowly, keeping the temperature below -20 °C. The solution was stirred for 15 min, then cooled to -50 °C. (Z)-Cyclooct-4-enecarboxylic acid 15 (54.0 g, 0.351 mol), dissolved in 150 mL THF, was added over a 20 min period at a temperature between -50 and -25 °C. The mixture was stirred for an additional 40 min, allowing the temperature to rise to -5 °C, and was subsequently heated for 3 h at 50 °C, after which it was cooled to -50 °C. Iodomethane (195.5 g, 1.377 mol) was added over a 20 min period at a temperature between -50 and -30 °C. The mixture was stirred overnight, heated for 1 h at 40 °C, and then concentrated in vacuo. Toluene (250 mL) was added to the residue, followed by 500 mL dilute hydrochloric acid. The phases were separated and the organic phase was washed with 100 mL 2 N hydrochloric acid. The aqueous phases were extracted with 2×250 mL toluene. The combined organic phase was concentrated in vacuo. The residue was purified by Kugelrohr distillation to yield 59.4 g of the methylated acid 16 as a colorless oil (0.353 mol, 100%), which was used as such in the next step. ¹H NMR (CDCl₃): δ = 5.75–5.60 (m, 1H), 5.55–5.40 (m, 1H), 2.4–1.5 (m, 10H), 1.27 (s, 3H). ¹³C NMR (CDCl₃): δ = 185.5 (C=O), 131.9 (=CH), 126.5 (=CH),

46.2, 35.3, 32.3, 27.1 (CH₃), 26.1, 24.8, 24.7. HRMS (ESI, *m/z*): Calcd for C₁₀H₁₇O₂⁺ ([M+H]⁺): 169.1223, Found: 169.1226.

(Z)-1-Methyl-7-oxabicyclo[4.2.2]dec-4-en-8-one (18). Compound 16 (42.0 g, 0.25 mol) in 300 mL dichloromethane was combined with 300 mL water and sodium bicarbonate (68.9 g, 0.82 mol). The mixture was stirred for 10 min and then cooled in ice. A mixture of potassium iodide (125.2 g, 0.754 mol) and iodine (129.0 g, 0.508 mol) was added over 1 h in 6 equal portions. The reaction mixture was stirred for 3.5 h and subsequently sodium bisulfite was added slowly, until mixture decoloration. The phases were separated and the cloudy aqueous phase was extracted with 2 × 250 mL dichloromethane. Drying and rotary evaporation gave the desired crude iodolactone 17 as a colorless oil. ¹H NMR (CDCl₃, product signals): δ = 5.65–5.5 (m, 2H), 4.8 (dt, 1H), 3.95 (dt, 1H), 2.6–1.95 (m, 8H). HRMS (ESI, *m/z*): Calcd for C₁₀H₁₆IO₂⁺ ([M+H]⁺): 295.0189, Found: 295.0189.

Compound 17 was dissolved in 250 mL toluene and DBU (65.2 g, 0.428 mol) was added. The mixture was allowed to stand overnight, after which it was heated under reflux for 75 min, at which point NMR indicated full conversion. After cooling, the reaction mixture was washed with 150 and 100 mL water. The combined aqueous phases were extracted with 250 mL toluene. The organic phase was dried and the residue was purified by Kugelrohr distillation to yield 38.9 g of the bicyclic olefin 18 as a colorless oil (0.234 mol, 94%). ¹H NMR (CDCl₃): δ = 5.95–5.85 (m, 1H), 5.45–5.35 (dm, 1H), 5.05 (bs, 1H), 2.5–2.3 (m, 1H), 2.2–2.0 (m, 2H), 1.95–1.6 (m, 5H), 1.27 (s, 3H). ¹³C NMR (CDCl₃): δ = 177.2 (C=O), 129.1 (=CH), 127.9 (=CH), 79.2 (CH), 45.2, 43.0, 31.9, 29.5 (CH₃), 26.6, 24.0. HRMS (ESI, *m/z*): Calcd for C₁₀H₁₅O₂⁺ ([M+H]⁺): 167.1067, Found: 167.1065.

Methyl (Z)-6-hydroxy-1-methylcyclooct-4-ene-1-carboxylate (19). Compound 18 (40.4 g, 0.243 mol) in 250 mL methanol and potassium bicarbonate (100.0 g, 1.0 mol) was stirred for 64 h at 28 °C, followed by filtration, washing with methanol, and rotary evaporation. The residue was chromatographed on 200 g silica using dichloromethane and subsequently dichloromethane/methanol as the eluent, affording pure 19 as a colorless oil (17.5 g, 0.117 mmol, 48%). ¹H NMR (CDCl₃): δ = 5.6–5.5 (m, 1H), 5.35–5.25 (m, 1H), 5.0–4.85 (m, 1H), 3.63 (s, 3H), 2.90 (d, 1H, OH), 2.35–1.90 (m, 5H), 1.75–1.45 (m, 3H), 1.20 (s, 3H). ¹³C NMR (CDCl₃): δ = 178.8 (C=O), 132.7 (=CH), 129.0 (=CH), 68.0 (CH), 52.0 (CH₃), 46.1, 35.9, 33.7, 30.4, 26.8, 24.7 (CH₃). HRMS (ESI, *m/z*): Calcd for C₁₁H₁₇O₂⁺ ([M-H₂O+H]⁺): 181.1223, Found: 181.1226.

Methyl (E)-6-hydroxy-1-methylcyclooct-4-ene-1-carboxylate (20a,b). Compound 19 (26.5 g, 133.8 mmol) was mixed with 25.0 g methyl benzoate and 1 L heptane/ether (4:1). The solution was irradiated, the irradiated solution being continuously flushed for 100 h through a silver nitrate impregnated silica column (213.6 g, containing ca. 126 mmol silver nitrate). Then, the silica column was successively flushed with 600 mL TBME, 500 mL TBME/5% methanol, 500 mL TBME/10% methanol, and 500 mL TBME/20% methanol. The first 3 eluates were concentrated in vacuo. The first eluate contained methyl benzoate and the starting hydroxy ester 19. The residues from the second and third eluate were combined, dissolved in TBME, and washed with 300 mL 10% ammonia solution. Drying in vacuo gave a residue that consisted of the axial/equatorial isomers (with respect to the hydroxy group) of

the *trans*-cyclooctene 20a,b in a ratio of ca. 5:4. The fourth eluate was washed with 300 mL 10% ammonia solution and then dried in vacuo affording a mixture of 20a,b (axial/equatorial ratio ca. 5:4). The residual column material was stirred with TBME, 100 mL water, and 300 mL 10% ammonia solution. Filtration, layer separation, and drying in vacuo gave a residue. The process was repeated twice to give a colorless oil that consisted of the axial/equatorial isomers of the *trans*-cyclooctenes (20a,b) in a ratio of ca. 1:7. All fractions of 20a,b were combined to give a total yield of 19.1 g (96.5 mmol, 72%). ¹H NMR (500 MHz, CDCl₃) (mixture of isomers): equatorial isomer: δ = 5.79 (ddd, *J* = 16.0, 11.8, 4.0 Hz, 1H), 5.37 (dd, *J* = 16.0, 9.6 Hz, 1H), 4.21 (td, *J* = 9.6, 5.6 Hz, 1H), 3.73 (s, 3H), 2.72 (qd, *J* = 11.8, 4.6 Hz, 1H), 2.25 (ddt, *J* = 14.4, 4.1, 2.0 Hz, 1H), 2.18–2.00 (m, 2H), 1.93 (dddd, *J* = 14.1, 11.9, 10.2, 1.5 Hz, 1H), 1.84 (s, 1H), 1.82–1.71 (m, 1H), 1.52 (ddd, *J* = 14.2, 12.5, 4.8 Hz, 1H), 1.31 (ddd, *J* = 15.5, 12.2, 1.5 Hz, 1H), 1.20 (s, 3H). ¹³C NMR (125 MHz, CDCl₃): δ = 177.22, 135.77, 132.54, 74.90, 51.27, 47.40, 45.87, 39.82, 38.77, 34.62, 30.88. ¹H NMR (CDCl₃) (mixture of isomers): axial isomer: δ = 6.05 (m, 1H), 5.6 (dd, 1H), 4.45 (bs, 1H), 3.62 (s, 3H), 2.35–1.7 (m, 8H), 1.5 (m, 1H), 1.08 (s, 3H). ¹³C NMR (CDCl₃): δ = 180.7 (C=O), 135.2 (=CH), 130.3 (=CH), 69.6 (CH), 52.1 (CH₃), 44.9, 44.7, 38.3, 30.9, 29.8, 18.3 (CH₃). HRMS (ESI, *m/z*): Calcd for C₁₁H₁₇O₂⁺ ([M-H₂O+H]⁺): 181.1223, Found: 181.1223.

Note: The axial/equatorial assignment is based on the stereochemistry of the hydroxy group, in similar fashion as for *trans*-cycloocten-2-ol. In both isomers the hydroxy and methyl ester substituents are positioned *cis* relative to each other. Consequently, in the axial isomer (20a) the hydroxyl group is in axial position and the methyl ester is in equatorial position, and vice versa, in the equatorial isomer (20b), hydroxyl group is in equatorial position and the methyl ester is in axial position. For the latter compound, which was obtained pure as described in the next section, this was evidenced by a detailed NMR-study using ¹H NMR, ¹³C NMR, COSY, HSQC, and NOESY (Supporting Information).

rel-(1R,4E,6R,PS)-6-Hydroxy-1-methylcyclooct-4-ene-1-carboxylic acid (axial isomer 21a). A solution of 1.60 g potassium hydroxide in 5 mL water was added over a 5 min period to a water-cooled solution of the *trans*-cyclooctene ester 20a,b isomer mixture (0.49 g, 2.47 mmol, ratio of the axial/equatorial isomer ca. 2.5:1 for this particular batch) in 11 mL methanol. The solution was stirred for 18 h at 28 °C. 15 mL water was added and the mixture was extracted with 2 × 30 mL TBME. The combined organic layers were washed with 10 mL water and then dried in vacuo to give the nonhydrolyzed equatorial ester 20b. The combined aqueous layers were treated with 30 mL TBME, and then with 4.5 g citric acid. The layers were separated and the aqueous layer was extracted with 30 mL TBME. The combined organic layers were dried and rotary evaporated at 55 °C to afford 0.34 g (1.85 mmol, 75%) of the pure axial isomer 21a of the *trans*-cyclooctene acid as a colorless oil. ¹H NMR (CDCl₃): δ = 6.15–5.95 (m, 1H), 5.6 (d, 1H), 4.45 (bs, 1H), 2.4–1.7 (m, 7H), 1.6 (dd, 1H), 1.18 (s, 3H). ¹³C NMR (CDCl₃): δ = 185.4 (C=O), 134.8 (=CH), 130.7 (=CH), 69.8 (CH), 44.8, 38.2, 31.0, 29.8 (CH₂), 18.1 (CH₃). Due to its limited stock stability compound 21a was converted to 22a and stored for further use.

Note: The hydrolysis of the axial/equatorial ester appears to be extremely selective. Whereas the equatorial ester in 20a hydrolyzes surprisingly easily at RT, the axial ester in 20b

remains unaffected, thus enabling a straightforward separation between both isomers. The axial ester hydrolyzes upon overnight heating at ca. 60 °C.

rel-(1*R*,4*E*,6*R*,*pS*)-2,5-Dioxopyrrolidin-1-yl-6-(((2,5-dioxopyrrolidin-1-yl)oxy)carbonyloxy)-1-methylcyclooct-4-ene-1-carboxylate (axial isomer **22a).** To a solution of compound **21a** (375 mg, 2.04 mmol) in 10.1 g MeCN was added DIPEA (1.95 g, 15.07 mmol), followed by *N,N'*-disuccinimidyl carbonate (2.25 g, 8.79 mmol). The mixture was stirred for 3 days at RT, and subsequently evaporated in vacuo at 55 °C. The residue was chromatographed on 20 g silica, with dichloromethane as eluent, followed by elution with dichloromethane containing an increasing amount of TBME (5–20%). The product fractions were combined and dried in vacuo. The resulting residue was stirred with TBME until a homogeneous suspension was obtained. Filtration and washing gave 400 mg of product **22a** as a white solid (0.95 mmol; 46%); mp 162 °C. ¹H NMR (CDCl₃): δ = 6.07 (ddd, *J* = 16.8, 10.7, 3.5 Hz, 1H), 5.62 (dd, *J* = 16.7, 2.5 Hz, 1H), 5.25 (s, 1H), 2.83 (2s, 8H), 2.5–2.25 (m, 4H), 2.2–1.9 (m, 4H), 1.28 (s, 3H). ¹³C NMR (125 MHz, CDCl₃): δ = 174.03, 169.16, 168.53, 150.61, 132.97, 128.80, 78.76, 44.33, 44.30, 35.69, 30.71, 30.09, 25.62, 25.47, 17.94. NOESY (Supporting Information) evidenced the equatorial orientation of the NHS ester, and axial orientation of the NHS carbonate. HRMS (ESI, *m/z*): Calcd for C₁₉H₂₂N₂O₉Na⁺ ([*M*+Na]⁺): 445.1218, Found: 445.1232.

NHS-TCO-Doxorubicin (Axial Isomer **23a).** Doxorubicin hydrochloride (133 mg; 2.30 × 10⁻⁴ mol) and **22a** (97.0 mg; 2.30 × 10⁻⁴ mol) were dissolved in DMF (5 mL), and DIPEA (148 mg; 1.15 × 10⁻³ mol) was added. The solution was stirred under an atmosphere of argon at 20 °C for 18 h. MeCN (6.5 mL), formic acid (0.2 mL), and water (6.5 mL), were added and the suspension was filtered. The filtrate was purified by preparative RP-HPLC (50% MeCN in water, containing 0.1% formic acid). The product was isolated by lyophilization, dissolved in chloroform (3 mL), and precipitated in diethyl ether (20 mL), to yield **23a** as an orange powder (134 mg; 68%); mp 179 °C. ¹H NMR (CDCl₃): δ = 13.97 (s, 1H), 13.22 (s, 1H), 8.03 (d, *J* = 7.9 Hz, 1H), 7.78 (t, *J* = 8.0 Hz, 1H), 7.38 (d, *J* = 8.6 Hz, 1H), 5.85 (m, 1H), 5.59 (m, 1H), 5.51 (s, 1H), 5.29 (s, 1H), 5.16 (d, *J* = 8.4 Hz, 1H), 5.12 (s, 1H), 4.75 (d, *J* = 4.8 Hz, 2H), 4.52 (d, *J* = 5.8 Hz, 1H), 4.15 (q, *J* = 6.5 Hz, 1H), 4.08 (d, *J* = 3.6 Hz, 3H), 3.87 (m, 1H), 3.69 (m, 1H), 3.26 (d, *J* = 18.8 Hz, 1H), 3.00 (m, 2H), 2.81 (s, 4H), 2.4–1.7 (br. m, 13H), 1.62 (s, 2H), 1.30 (d, *J* = 6.5 Hz, 3H), 1.23 (s, 3H) ppm. ¹³C NMR (CDCl₃): δ = 213.89, 187.07, 186.68, 174.30, 169.27, 161.03, 156.15, 155.64, 154.66, 135.73, 135.49, 133.58, 131.70, 131.10, 120.88, 119.83, 118.43, 111.58, 111.40, 100.73, 72.09, 69.65, 67.28, 65.54, 56.67, 46.87, 44.38, 35.75, 34.00, 30.49, 30.39, 30.20, 25.61, 17.92, 16.84 ppm. HRMS (ESI, *m/z*): Calcd for C₄₂H₄₆N₂O₁₇Na⁺ ([*M*+Na]⁺): 873.2694, Found: 873.2681.

CC49-TCO-Dox (12) Preparation. Typically, 1.25 mg CC49 (5 mg/mL solution in PBS) was reacted with 40 molar equiv of NHS-TCO-Dox (**23a**, 0.29 μmol in 21.3 μL DMF) in a total volume of 330 μL PBS/propylene glycol/DMF (70:20:10% v/v). The pH was adjusted to 9 with 1 M sodium carbonate buffer. The reaction was carried out under agitation for 2 h at RT in complete darkness. Subsequently, the TCO-Dox-modified mAb (**12**) was washed with PBS/propylene glycol/DMF (three times) and PBS/propylene glycol (75:25% v/v, three times) using an Amicon Ultra-15 centrifugal device (50 kDa MW cutoff). This procedure afforded an average 2.0–

2.6 TCO–Dox groups per antibody, as determined by UV-absorbance at 280 and 480 nm and with a tetrazine titration. SEC HPLC and SDS-PAGE of solutions of **12** showed the presence of a monomeric species with minimal aggregates. The solutions were stored at +4 °C in complete darkness. At various times the amount of reactive TCO present in solution was assayed with a tetrazine titration (4 different batches of **12** for over one year). At various times solutions of **12** were analyzed by SEC-HPLC with UV detection at 260 nm (proteins) and 480 nm (Dox) and no free Dox was found.

Doxorubicin Release from CC49-TCO-Dox in Vitro.

The absolute Dox release from **12** upon addition activator **3** was measured by SEC-HPLC. Construct **12** (150 μg) was mixed with **3** (100 equiv tetrazine to TCO) in PBS (200 μL total) and incubated at 37 °C on a thermomixer (350 rpm) in complete darkness. At 1, 3, and 24 h an aliquot of the reaction mixture was analyzed by SEC with UV detection at 260 nm (protein) and 480 nm (Dox). The % release Dox was estimated from the A₄₈₀/A₂₆₀ area ratio for the mAb peak. Native CC49 (corresponding to 100% release) and unreacted **12** (0% release) were used as controls. The experiment was performed in triplicate.

The extent of Dox release in the presence of the activators **3–6** was evaluated by RP-HPLC. Construct **12** (75 μg) was mixed with a fixed amount of activator (100 equiv tetrazine to TCO) and daunorubicin (Daun, 200 ng, as internal standard) in PBS or 50% MS in PBS (0.5 mL total volume). Solutions containing **12** and Daun but no activator were used as controls. The mixtures were incubated at 37 °C in complete darkness and, at various times, aliquots were withdrawn, 2-fold diluted with ice-cold MeCN, and vortexed (10 s). After centrifugation (5 min, 12 000 rpm), the supernatants were 4-fold diluted with PBS and analyzed by RP-HPLC using a fluorescence detector. All experiments were carried out in triplicate. The % Dox released at each time point was calculated from the Dox/Daun peak area ratio in the fluorescence chromatogram and the mAb/Daun concentration in each mixture. Calibration curves were obtained using PBS/MS solutions containing known amounts of Dox and Daun which were incubated at 37 °C and analyzed by RP-HPLC at various times. Only the peaks of intact Dox (*R_t* = 5.8 min) and Daun (*R_t* = 11.0 min) were used for the calculations.

The amount of residual free (unreacted) TCO in the **12**/activator mixtures was evaluated after 1 and 3 h incubation in PBS at 37 °C. Aliquots of the reaction mixtures were added with a known excess (10 equiv to initial TCO) of the highly reactive ¹⁷⁷Lu-**14** and further incubated at 37 °C for 20 min. After incubation, the mixtures were analyzed by SDS-PAGE on 4–15% gradient gels followed by phosphor imager. The amount of free TCO in each solution at the time of ¹⁷⁷Lu-**14** addition was estimated from the % radioactivity in the mAb region of each lane. Each experiment was performed in triplicate. A solution of **12** in PBS incubated for 1 h at 37 °C without activator and then reacted with ¹⁷⁷Lu-**14** was used to determine the 100% unreacted TCO.

Radiochemistry and Immunoreactivity. The DOTA-tetrazine **14** and CC49-TCO-Dox **12** were labeled with ¹⁷⁷Lu and ¹²⁵I, respectively, as previously described.²¹ Carrier-added ¹⁷⁷Lu-**14** was used in vitro while noncarrier-added ¹⁷⁷Lu-**14** was used for animal experiments. After radiolabeling and size exclusion purification (¹²⁵I-**12**), all radiolabeled species showed >99% label incorporation and >95% radiochemical purity, as confirmed by iTLC, HPLC, and SDS-PAGE.

CC49-TCO-Dox (**12**, 10 μg) was labeled directly with ^{125}I (Bolton-Hunter procedure, statistically labeling the entire mAb population) or indirectly with ^{177}Lu (reaction with 1 equiv ^{177}Lu -**14**, labeling only the TCO-functionalized mAb) and then reacted with 20 equiv bovine submaxillary mucin (BSM, a soluble TAG72 positive mucin; ca. 4000 kDa MW) in 1% bovine serum albumin (BSA) in PBS solution (60 μL total). $^{125}\text{I}/^{177}\text{Lu}$ -**12** incubated in 1% BSA in PBS was used as control. After 30 min incubation at 37 $^{\circ}\text{C}$, SEC-HPLC analysis of the $^{125}\text{I}/^{177}\text{Lu}$ -**12**/BSM mixtures showed a shift of the radioactive peak at lower retention time with respect to that observed for the $^{125}\text{I}/^{177}\text{Lu}$ -**12**/BSA mixtures, thus confirming binding of **12** to BSM, i.e., complete retention of immunoreactivity upon CC49-TCO-Dox conjugation and radiolabeling.

Note: ^{125}I and ^{177}Lu emit ionizing radiation (β^{-} and/or γ): researchers must handle them according to the guidelines set forth by their institution and national nuclear regulatory commission and follow ALARA (As Low As Reasonably Achievable) protocols to minimize exposure.

Animal Experiments. All animal experiments were performed according to the principles of laboratory animal care (NIH publication 85–23, revised 1985) and the Dutch national law “Wet op de Dierproeven” (Stb 1985, 336). The *in vivo* experiments were performed in tumor-free or tumor-bearing nude female Balb/C mice (20–25 g body weight, Charles River Laboratories). The human colon cancer cell line LS174T was obtained from the ATCC and maintained in Eagle’s minimal essential medium (Sigma) supplemented with 10% heat inactivated fetal calf serum (Gibco), penicillin (100 U/mL), streptomycin (100 $\mu\text{g}/\text{mL}$), and 2 mM GlutaMax. Mice were inoculated subcutaneously with 3×10^6 cells in 100 μL sterile PBS and were used 7–10 days after tumor inoculation, when the tumors reached approximately 70–200 mm^3 size. At the end of each experiment the mice were anesthetized and euthanized by cervical dislocation. Blood was withdrawn by heart puncture and selected organs and tissues (including full stomachs and intestines) were harvested, blotted dry, and weighed. The tumors were counted immediately for radioactivity and then frozen at -80°C for Dox extraction. The remaining organs and tissues were added with 1 mL PBS and then measured for radioactivity. The sample radioactivity was counted in a gamma counter (Wizard 1480, PerkinElmer) along with standards to determine the % injected dose per gram (%ID/g) and the % injected dose per organ (%ID/organ). The tissues from single-isotope experiments were measured using 10–80 keV energy window for ^{125}I . All other samples were measured using dual-isotope protocol (10–80 keV and 155–380 keV energy windows for ^{125}I and ^{177}Lu , respectively) with cross-contamination correction.

CC49-TCO-Dox Blood Kinetics and *In Vivo* TCO Stability. One group of 3 tumor-free mice was administered 100 μg ^{125}I -**12** (ca. 0.35 MBq/100 μL per mouse) and at selected time points (5 min, and 3, 6, 24, 48, and 72 h) blood samples (ca. 20 μL) were withdrawn from the vena saphena. Four days post-mAb injection the mice were euthanized, blood was withdrawn by heart puncture and organs and tissues of interest were harvested and counted in a gamma-counter. One more group of 3 tumor-free mice was administered 300 μg ^{125}I -**12** (ca. 0.65 MBq/100 μL per mouse) and at selected time points (1, 3, 6, 24, 48, 72, and 96 h) 50–60 μL blood samples were withdrawn and transferred into vials containing heparin (5 μL). These blood samples were used to assess the TCO

stability *in vivo*, as previously described.¹¹ At the end of the evaluation, the mice were euthanized, and the ^{125}I -activity in stomachs and thyroids was measured. The low values found in these organs ($0.14 \pm 0.02\%$ ID in stomachs and $0.43 \pm 0.07\%$ ID in thyroids) confirms the absence of ^{125}I -**12** *in vivo* dehalogenation.

Tumor Blocking Experiments. Groups of LS174T xenografted mice ($n = 3-4$) were injected with ^{125}I -**12** (5 mg/kg, corresponding to 36–47 μg Dox/kg; 0.2–0.4 MBq per mouse; $t = 0$) followed by a clearing agent²¹ (8 mg/kg; $t = 24$ h). Twenty-six hours post-mAb injection, the mice were administered activators 3–6 (1 \times dose = 33.5 μmol tetrazine/kg; 10 \times dose = 0.335 mmol tetrazine/kg) via different routes (bolus injection through the lateral tail vein or intraperitoneal injection) followed 1 h later by ^{177}Lu -**14** (0.335 μmol tetrazine/kg; ca. 1.5 MBq per mouse). One group of mice (“no ADC” group; $n = 4$) received ^{125}I -CC49 ($t = 0$) followed by ^{177}Lu -**14** ($t = 27$ h). Another group of mice (“no activator” group; $n = 6$) received ^{125}I -**12** (5 mg/kg) followed by clearing agent ($t = 24$ h) and ^{177}Lu -**14** ($t = 27$ h). Three hours after ^{177}Lu -**14** administration all mice were anesthetized with isoflurane and euthanized and blood and tissue samples were collected. One group of mice ($n = 3$) received only ^{125}I -**12** and was euthanized 30 h post-mAb injection for control Dox release (tumor extraction).

Dox Extraction from Tissue Samples. To determine the amount of antibody-released Dox present in tumors, tumor samples were spiked with Daun as internal standard and subsequently homogenized and extracted following a published procedure with minor adaptations.³⁰ Specifically, the tumor samples were combined with 1.2–1.5 mL water, 15 ng Daun, and a 5 mm stainless steel bead (Qiagen). The samples were subsequently homogenized at 4 $^{\circ}\text{C}$ at 30 Hz for 20 min using a tissue lyser (Qiagen). Tumor homogenates were incubated with 600 μL of a 33% w/v stock AgNO_3 in water for 10 min and subsequently extracted with 9 mL chloroform:isopropanol (2:1 v/v) in glass culture tubes (DURAN), by vigorous mixing for 2 min. The samples were centrifuged at 1800 $\times g$ for 10 min at RT and the organic phase was isolated using a phase separation column (Chromabond PTS) and subsequently evaporated at 40 $^{\circ}\text{C}$ in a glass test tube (DURAN) in a block heater under a gentle nitrogen flow. The dried residue was dissolved in 140 μL 25% MeCN in water (with 0.1% TFA) and centrifuged at 12 000 rpm for 10 min at RT. The supernatant (100 μL) was analyzed by RP-HPLC with fluorescence detector. A calibration curve was prepared with samples containing known amounts of Dox and Daun in water which were extracted following the same procedure used for tumors. Only the peaks of intact Dox and Daun were used for the calculations.

Data Analysis. The data are presented as mean %ID/g or % ID/organ \pm one standard deviation (SD). Curve fitting, area-under-the-curve calculations, one-way ANOVA and Dunnett’s post-tests were performed with GraphPad Prism v 5.01. The difference between two data points was considered statistically significant when $P < 0.05$.

■ ASSOCIATED CONTENT

📄 Supporting Information

The Supporting Information is available free of charge on the ACS Publications website at DOI: 10.1021/acs.bioconjchem.6b00231.

General procedures, additional syntheses, LC-MS, RP-HPLC, SEC-HPLC and SDS-PAGE analyses, NMR spectra, and biodistribution data (PDF)

AUTHOR INFORMATION

Corresponding Author

*E-mail: marc.robillard@tagworkspharma.com. Phone: +31402748264.

Notes

The authors declare the following competing financial interest(s): Co-founder of Tagworks Pharmaceuticals.

ACKNOWLEDGMENTS

We thank Caren van Kammen and Carlijn van Helvert (Maastricht University) for support with animal experiments and Ellen M. H. Schmitz and Xianwen Lou (Technical University Eindhoven) for support with MS analysis. This research was supported by NanoNextNL (The Netherlands, Grant 03C.3).

ABBREVIATIONS

%ID/g, percent injected dose per gram; %ID/organ, percent injected dose per organ; ADC, antibody–drug conjugate; BSA, bovine serum albumin; BSM, bovine submaxillary mucin; Daun, daunorubicin; DOTA, 1,4,7,10-tetraazacyclododecane-1,4,7,10-tetraacetic acid; Dox, doxorubicin; IEDDA, inverse-electron-demand Diels–Alder; MS, mouse serum; TCO, *trans*-cyclooctene

REFERENCES

- (1) Polakis, P. (2016) Antibody Drug Conjugates for Cancer Therapy. *Pharmacol. Rev.* 68, 3–19.
- (2) Sapra, P., Hooper, A. T., O'Donnell, C. J., and Gerber, H.-P. (2011) Investigational antibody drug conjugates for solid tumors. *Expert Opin. Invest. Drugs* 20, 1131–1149.
- (3) Grana, C., Chinol, M., Robertson, C., Mazzetta, C., Bartolomei, M., De Cicco, C., Fiorenza, M., Gatti, M., Caliceti, P., and Paganelli, G. (2002) Pretargeted adjuvant radioimmunotherapy with Yttrium-90-biotin in malignant glioma patients: A pilot study. *Br. J. Cancer* 86, 207–212.
- (4) Hofmeister, V., Schrama, D., and Becker, J. C. (2008) Anti-cancer therapies targeting the tumor stroma. *Cancer Immunol. Immunother.* 57, 1–17.
- (5) Perrino, E., Steiner, M., Krall, N., Bernardes, G. J. L., Pretto, F., Casi, G., and Neri, D. (2014) Curative Properties of Noninternalizing Antibody–Drug Conjugates Based on Maytansinoids. *Cancer Res.* 74, 2569–2578.
- (6) Rossin, R., and Robillard, M. S. (2014) Pretargeted imaging using bioorthogonal chemistry in mice. *Curr. Opin. Chem. Biol.* 21, 161–169.
- (7) Blackman, M. L., Royzen, M., and Fox, J. M. (2008) Tetrazine Ligation: Fast Bioconjugation Based on Inverse-Electron-Demand Diels–Alder Reactivity. *J. Am. Chem. Soc.* 130, 13518–13519.
- (8) Thalhammer, F., Wallfaher, U., and Sauer, J. r. (1990) Reaktivität einfacher offenkettiger und cyclischer dienophile bei Diels–Alderreaktionen mit inversem elektronenbedarf. *Tetrahedron Lett.* 31, 6851–6854.
- (9) Genady, A. R., Tan, J., El-Zaria, M. E., Zlitni, A., Janzen, N., and Valliant, J. F. (2015) Synthesis, characterization and radiolabeling of carborane-functionalized tetrazines for use in inverse electron demand Diels–Alder ligation reactions. *J. Organomet. Chem.* 791, 204–213.
- (10) Meyer, J.-P., Houghton, J. L., Kozlowski, P., Abdel-Atti, D., Reiner, T., Pillarsetty, N. V. K., Scholz, W. W., Zeglis, B. M., and Lewis, J. S. (2016) ¹⁸F-Based Pretargeted PET Imaging Based on Bioorthogonal Diels–Alder Click Chemistry. *Bioconjugate Chem.* 27, 298–301.

(11) Rossin, R., van Duijnhoven, S. M. J., Läppchen, T., van den Bosch, S. M., and Robillard, M. S. (2014) Trans-Cyclooctene Tag with Improved Properties for Tumor Pretargeting with the Diels–Alder Reaction. *Mol. Pharmaceutics* 11, 3090–3096.

(12) van Duijnhoven, S. M. J., Rossin, R., van den Bosch, S. M., Wheatcroft, M. P., Hudson, P. J., and Robillard, M. S. (2015) Diabody Pretargeting with Click Chemistry In Vivo. *J. Nucl. Med.* 56, 1422–1428.

(13) Zeglis, B. M., Brand, C., Abdel-Atti, D., Carnazza, K. E., Cook, B. E., Carlin, S., Reiner, T., and Lewis, J. S. (2015) Optimization of a Pretargeted Strategy for the PET Imaging of Colorectal Carcinoma via the Modulation of Radioligand Pharmacokinetics. *Mol. Pharmaceutics* 12, 3575–3587.

(14) Versteegen, R. M., Rossin, R., ten Hoeve, W., Janssen, H. M., and Robillard, M. S. (2013) Click to Release: Instantaneous Doxorubicin Elimination upon Tetrazine Ligation. *Angew. Chem., Int. Ed.* 52, 14112–14116.

(15) Khan, I., Agris, P. F., Yigit, M. V., and Royzen, M. (2016) In situ activation of a doxorubicin prodrug using imaging-capable nanoparticles. *Chem. Commun.* 52, 6174–6177.

(16) Li, J., Jia, S., and Chen, P. R. (2014) Diels–Alder reaction–triggered bioorthogonal protein decaging in living cells. *Nat. Chem. Biol.* 10, 1003–1005.

(17) Zhang, G., Li, J., Xie, R., Fan, X., Liu, Y., Zheng, S., Ge, Y., and Chen, P. R. (2016) Bioorthogonal Chemical Activation of Kinases in Living Systems. *ACS Cent. Sci.* 2, 325.

(18) Agustin, E., Asare Okai, P. N., Khan, I., Miller, M. R., Wang, R., Sheng, J., and Royzen, M. (2016) A fast click-slow release strategy towards the HPLC-free synthesis of RNA. *Chem. Commun.* 52, 1405–1408.

(19) Forero-Torres, A., Shen, S., Breitz, H., Sims, R. B., Axworthy, D. B., Khazaeli, M. B., Chen, K.-H., Percent, I., Besh, S., and LoBuglio, A. F. (2005) Pretargeted Radioimmunotherapy (RIT) with a Novel Anti-TAG-72 Fusion Protein. *Cancer Biother. Radiopharm.* 20, 379–390.

(20) Meredith, R., Shen, S., Macey, D., Khazaeli, M. B., Carey, D., Robert, F., and LoBuglio, A. (2003) Comparison of Biodistribution, Dosimetry, and Outcome from Clinical Trials of Radionuclide-CC49 Antibody Therapy. *Cancer Biother. Radiopharm.* 18, 393–404.

(21) Rossin, R., Läppchen, T., van den Bosch, S. M., Laforest, R., and Robillard, M. S. (2013) Diels–Alder Reaction for Tumor Pretargeting: In Vivo Chemistry Can Boost Tumor Radiation Dose Compared with Directly Labeled Antibody. *J. Nucl. Med.* 54, 1989–1995.

(22) Rossin, R., Renart Verkerk, P., van den Bosch, S., Vulderson, R., Verel, I., Lub, J., and Robillard, M. (2010) In Vivo Chemistry for Pretargeted Tumor Imaging in Live Mice. *Angew. Chem., Int. Ed.* 49, 3375–3378.

(23) Rossin, R., van den Bosch, S. M., ten Hoeve, W., Carvelli, M., Versteegen, R. M., Lub, J., and Robillard, M. S. (2013) Highly Reactive *trans*-Cyclooctene Tags with Improved Stability for Diels–Alder Chemistry in Living Systems. *Bioconjugate Chem.* 24, 1210–1217.

(24) Wagner, J. A., Mercadante, D., Nikić, I., Lemke, E. A., and Gräter, F. (2015) Origin of Orthogonality of Strain-Promoted Click Reactions. *Chem. - Eur. J.* 21, 12431–12435.

(25) Nolting, B. Linker Technologies for Antibody–Drug Conjugates. In *Antibody-Drug Conjugates*, Ducry, L., Ed.; Humana Press: Totowa, NJ, 2013; Vol. 1045, pp 71–100.

(26) Erickson, H. K., Lewis Phillips, G. D., Leipold, D. D., Provenzano, C. A., Mai, E., Johnson, H. A., Gunter, B., Audette, C. A., Gupta, M., Pinkas, J., et al. (2012) The Effect of Different Linkers on Target Cell Catabolism and Pharmacokinetics/Pharmacodynamics of Trastuzumab Maytansinoid Conjugates. *Mol. Cancer Ther.* 11, 1133–1142.

(27) Alley, S. C., Zhang, X., Okeley, N. M., Anderson, M., Law, C.-L., Senter, P. D., and Benjamin, D. R. (2009) The Pharmacologic Basis for Antibody–Auristatin Conjugate Activity. *J. Pharmacol. Exp. Ther.* 330, 932–938.

(28) Devaraj, N. K., Thurber, G. M., Keliher, E. J., Marinelli, B., and Weissleder, R. (2012) Reactive polymer enables efficient in vivo

bioorthogonal chemistry. *Proc. Natl. Acad. Sci. U. S. A.* 109, 4762–4767.

(29) Bloodworth, A. J., Melvin, T., and Mitchell, J. C. (1988) Mechanistic aspects of oxygen transfer by gem-dialkylperoxonium ions. *J. Org. Chem.* 53, 1078–1082.

(30) de Smet, M., Heijman, E., Langereis, S., Hijnen, N. M., and Gröll, H. (2011) Magnetic resonance imaging of high intensity focused ultrasound mediated drug delivery from temperature-sensitive liposomes: An in vivo proof-of-concept study. *J. Contr. Rel.* 150, 102–110.